

Article

Real-Time Penetration Recognition Based on Voltage Signal in K-TIG Welding

Huizhong Bai, Na Ni, Yingna Wu, Rui Yang and Guangping Xie *

Center for Adaptive System Engineering, School of Creativity and Art, ShanghaiTech University, Shanghai 201210, China; baihz@shanghaitech.edu.cn (H.B.); nina@shanghaitech.edu.cn (N.N.); wuyn@shanghaitech.edu.cn (Y.W.); yangrui@shanghaitech.edu.cn (R.Y.)

* Correspondence: xiegp@shanghaitech.edu.cn

Abstract: This paper focuses on discerning the melting state of keyhole tungsten inert gas (K-TIG) welding, a promising welding technique still considered a novelty. In order to achieve this goal, a sensing system is established to collect voltage signals during the welding process of 304 stainless steel. Analysis of the collected signals reveals that the characteristic signal power spectrum between 36 kHz and 37 kHz is closely related to whether the welding has complete joint penetration. The experimental findings confirm that the spectral power density of the characteristic signal varies significantly with the alteration of welding quality. Moreover, it is observed that when the welding melting state remains unchanged, the change in welding parameters is not noteworthy. When adjusting welding parameters to maintain stable feature signals during the welding process, the corresponding penetration state of the welding does change. Therefore, it is possible to ensure the stability of welding quality by altering welding parameters in real time. These research results provide valuable insights into the real-time quality monitoring of the K-TIG welding process.

Keywords: K-TIG welding; welding quality; arc voltage; power spectrum; real-time monitoring



Citation: Bai, H.; Ni, N.; Wu, Y.; Yang, R.; Xie, G. Real-Time Penetration Recognition Based on Voltage Signal in K-TIG Welding. *Appl. Sci.* **2023**, *13*, 7412. <https://doi.org/10.3390/app13137412>

Academic Editor:
Abílio Manuel Pinho de Jesus

Received: 21 April 2023
Revised: 29 April 2023
Accepted: 5 May 2023
Published: 22 June 2023



Copyright: © 2023 by the authors. Licensee MDPI, Basel, Switzerland. This article is an open access article distributed under the terms and conditions of the Creative Commons Attribution (CC BY) license (<https://creativecommons.org/licenses/by/4.0/>).

1. Introduction

Keyhole tungsten inert gas (K-TIG) welding is a promising welding technology for deep penetration of medium and thick plate materials [1]. Developed by the Commonwealth Scientific and Industrial Research Organisation (CSIRO, Canberra, Australia) of the Australian government in 1997, K-TIG welding utilizes a high current to generate an arc with high energy, strong penetration force, and high stiffness, enabling it to weld metal materials directly without the need for grooving or filler wire [2]. By achieving single-side welding and double-side forming in one step, K-TIG welding significantly enhances welding efficiency while reducing welding costs [3,4]. Nonetheless, given the characteristic of K-TIG welding that achieves single-side welding and double-side forming in one step, ensuring its quality during the welding process is paramount.

The success of keyhole tungsten inert gas (K-TIG) welding relies heavily on the stability of the molten pool keyhole during the welding process. This stability is determined by a delicate balance between the arc pressure, the liquid surface of the back small hole, and the gravity of the metal [5]. The welding process is complex and characterized by non-equilibrium and instantaneous features. To ensure the stability and reliability of welding quality, it is essential to employ online welding quality evaluation technology [6–8]. This technology not only improves welding efficiency and productivity but also reduces the need for offline destructive or non-destructive testing methods. Current mainstream signal acquisition methods for online welding quality evaluation involve sound [9–11], spectral [12,13], current-voltage [14–17], and visual sensing methods [18–20].

However, the strong arc light generated by the high current (300–1000 A) of K-TIG welding makes it difficult to evaluate welding quality using visual methods. At the same time, practical limitations, such as the cost of visual acquisition equipment and

space requirements for welding platforms, make visual sensing methods challenging to implement [21]. As an alternative, acoustic sensing has been proposed due to its lower cost and easier installation. However, sound noise generated in actual factory production processes can make it difficult to denoise and obtain a pure arc sound [22]. In comparison, the arc electrical signal is closely linked to the welding process and is relatively easier to acquire. Therefore, this paper chooses to evaluate welding quality through the arc electrical signal. A novel method based on the arc electrical signal is proposed for online welding quality evaluation in K-TIG welding. The method involves collecting the arc electrical signal using a high-speed data acquisition system, followed by filtering and denoising the signal to remove unwanted noise. Subsequently, advanced signal processing techniques, including feature extraction and classification algorithms, are employed to analyze the signal and evaluate welding quality in real time. Experimental results demonstrate that the proposed method achieves high accuracy in evaluating welding quality in K-TIG welding, even in the presence of strong arc light interference; furthermore, this method has the advantages of low cost and easy installation compared to visual and acoustic sensing methods [23,24]. Therefore, the proposed method based on the arc electrical signal shows great potential for online welding quality evaluation in K-TIG welding applications.

Arc electrical signal sensing encompasses arc current, arc voltage, and plasma voltage discharged from the back. In order to enhance the penetrating ability and welding quality of keyhole plasma arc welding, a novel penetration closed-loop control system has been established by Cheng et al. [23]. This system chooses the welding current and plasma gas flow rate as the adjustable variables. Real-time detection of penetration status is achieved from the welding arc voltage using the wavelet method. A multi-sensor sensing system has been developed by Shi et al. [25] for the collection of voltage, current, and arc sound signals. A unique frequency peak has been discovered at 2–4 kHz, and its physical significance has been analyzed, indicating that it is related to the oscillation of the molten pool. Oscillation modes in the oscillation frequency of the molten pool have been extracted based on the algorithm, and different welding states have been analyzed to determine the specific mode for full penetration. Experiments have shown that the oscillation frequency between partial penetration and complete penetration differs. The combination of the identified frequency band and the proposed algorithm can be conveniently utilized to identify weld penetration.

This paper proposes a novel method for identifying complete joint penetration in K-TIG welding by extracting specific frequency band characteristics from the arc voltage signal. To establish an acquisition system for collecting voltage signals during the welding process, Section 2 presents the welding experiments. Section 3 then analyzes the physical significance of the feature frequency and presents the feature frequency. The intensity difference of the feature frequency signal between the incomplete joint penetration and complete joint penetration scenarios is distinct, thus enabling the determination of the weld penetration status to a certain extent. In Section 4, step-change speed experiments are conducted to validate the findings of Section 3. The results demonstrate the effectiveness of the proposed method for identifying complete joint penetration in K-TIG welding; specifically, the feature frequency analysis accurately distinguishes the penetration status. Finally, Section 5 presents the concluding remarks on the proposed method for identifying complete joint penetration in K-TIG welding based on the arc voltage signal. The experimental results show that the proposed method can effectively evaluate the welding quality and has the potential to be applied in practical production environments. The proposed method is a valuable contribution to the field of welding quality control, and further research could extend this method to other welding techniques and applications.

2. Materials and Methods

The experimental setup employed in this study is illustrated in Figure 1. It comprises four essential components: the K-TIG welding component, the programmable logic controller (PLC) motion component, the industrial personal computer (IPC) control system component, and the signal sensing component. The K-TIG welding component encom-

passes a DC welding power source, a cooling water supply system, and a specialized welding gun for K-TIG welding. The PLC motion component provides three degrees of freedom, facilitating control over the welding gun's movement. During the welding process, the current and voltage are measured by Hall sensors, which are protected by a protection circuit equipped with a differential amplifier. The IPC control system is responsible for acquiring data and adjusting welding parameters, while the National Instruments USB-6251-BNC acquisition card is employed to capture the current and voltage signals at a sampling frequency of 200 kHz. To attain different penetration states, two identical 304 austenitic stainless steel plates ($300 \times 150 \times 10$ mm) are assembled and utilized for the welding experiments. During the experiment, the two plates are brought together to create a gap of 0. Ar is used as the shielding gas with a flow rate of 20 L/min, while the CTWD was controlled at 3 mm, and the welding torch is facing the splicing part of the two plates.

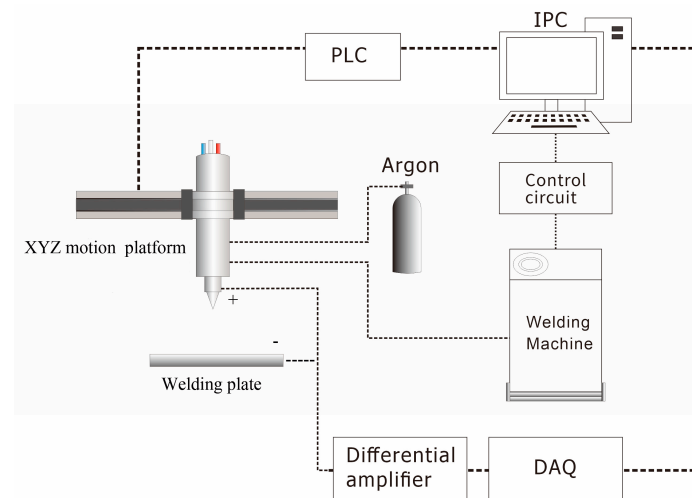


Figure 1. Schematic diagram of the welding experiment system.

The power supply used in the current research is an efficient deep penetration arc welding machine produced by Guangdong Fuweide Welding Co., Ltd., with the model K-TIG1000 (Guangdong Fuweide Welding Co., Ltd., Huizhou, China); the signal acquisition card is the National Instruments USB-6251-BNC (National Instruments, Austin, TX, USA). The PLC control system, XYZ motion platform, and IPC control system are developed by Shanghai Lianqing Power Technology Co., Ltd. (Shanghai Lianqing Power Technology Co., Ltd., Shanghai, China).

During the experiment, the gap between the welded plates is controlled to be zero, and the K-TIG welding technology is used to obtain a completely melted trial plate with a welding current of 525 A and a welding speed of 240 mm/min. To control variables and study different welding quality results, the researchers adjust another experimental parameter while keeping either the welding current or welding speed constant. The specific welding parameters are shown in Table 1.

Table 1. Test parameters.

Welding Parameters	Value (Speed)	Value (Current)
Welding current	525 A	450, 480, 500, 525, 550, 570, 600 A
Welding speed	160, 180, 200, 220, 240, 280, 300, 320, 360 mm/min	240 mm/min
Gap	0 mm	
CTWD	3 mm	
Flow rate	20 L/min	
Shielding gas	Pure argon (99.9%)	

The experimental results show that when the welding current was kept constant at 525 A, the arc could not completely melt the trial plate when the welding speed is increased to 300 mm/min. Similarly, when the welding speed is kept constant at 240 mm/min, the arc cannot completely melt the trial plate when the welding current is reduced to 500 A. Continuously increasing the welding speed or reducing the welding current to reduce the heat input on the surface of the welding trial plate will undoubtedly result in an incomplete melting outcome. However, within the window of the welding parameters, unstable welding quality is likely to occur, where the arc can sometimes penetrate the trial plate, while in other cases, it is unable to do so. Due to the strong arc light during the welding process, it is difficult for the welding personnel to directly observe the specific welding conditions. Therefore, in this experiment, the voltage between the tungsten electrode and the welding trial plate is collected and then amplified by the differential amplification circuit and collected and analyzed by the data acquisition card. The experimental procedures are conducted in strict accordance with scientific methods and procedures to ensure the accuracy and reliability of the results.

3. Experimental Results and Discussion

To ensure the safety of the acquisition card, a differential amplifier is utilized in the present study. Its role is to decrease the voltage by a factor of 1/200 of its original value proportionally. Figure 2a portrays the voltage time-domain signal acquired during the welding of 304 austenitic stainless steel with a welding current of 525 A and a welding speed of 240 mm/min. The voltage demonstrated a continuous rise from the arc initiation and ultimately stabilized after a certain duration of time. For this study's purpose, the signal analysis primarily focuses on the time period that excludes the arc initiation and termination phases. It is worth noting that the voltage's time domain signal is analyzed with meticulous care in this research.

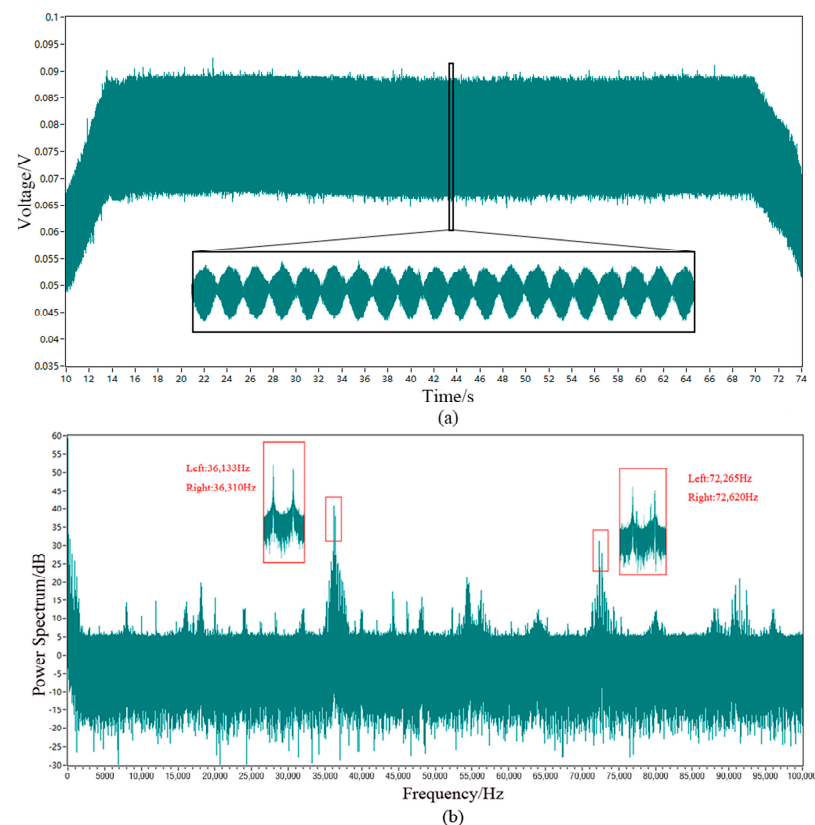


Figure 2. The time domain and frequency domain of the signal collected in the experiment. (a) Time domain; (b) frequency domain.

Figure 2b depicts the frequency domain signal of the 304 austenitic stainless steel experiment, revealing two prominent frequency bands: 36–37 kHz and 72–73 kHz. Within each band, two frequency peaks were evident, with frequencies of 36,133 Hz and 36,310 Hz being dominant and frequencies of 72,265 Hz and 72,620 Hz being harmonic. These frequency characteristics can be extracted from the voltage signal and utilized for further analysis.

3.1. Extraction of Characteristic Signal Intensity

In this section, the paper explores the correlation between the welding melt state and the characteristic signal strength in welding. To extract the characteristic signal strength of the frequency range of 36–37 kHz during the welding process, the paper takes the maximum value of the two similar frequency signal strengths of 36,133 Hz and 36,310 Hz, whose relative sizes are not fixed. Real-time monitoring of the welding melt state was achieved by selecting a data point as a sampling window and performing a fast Fourier transform in a sliding and stepping manner to calculate the characteristic signal strength of the frequency range of 36–37 kHz. The selection of the number of data points and the frequency of calculation are critical factors to consider. If the number of points is too small, the calculated characteristic signal amplitude by fast Fourier transform will be distorted, leading to incorrect trend reflection of the characteristic signal amplitude changes during the welding process. However, selecting too many data points will prolong the calculation time for the fast Fourier transform, slowing down the program's speed and rendering it incapable of meeting the real-time requirements. Figure 3 displays the monitoring of characteristic signal intensity under different sizes of data windows during the welding process: a welding current of 500 A and a welding speed of 240 mm/min. It can be observed that the characteristic signal intensity calculated from a small data window had difficulty in displaying the variation of signal intensity throughout the welding process. Selecting a large window not only increases the computational load of the fast Fourier transform and prolongs the calculation time but also reduces the sensitivity of signal monitoring to some extent. Therefore, in this study, a data window of 1 million data points was chosen, which calculates 5 s of data points simultaneously to select the data window size.

The sliding step size plays a crucial role in the real-time monitoring of the welding process, as it affects the response rate of signal tracking and the closed-loop control capability of the system. In practical applications, a smaller step size is welcomed, enabling the system to capture welding defect signals and initiate prompt corrective measures. Figure 4 displays the monitoring of characteristic signal intensity under different step sizes during the welding process while choosing a window size of 1 million. It proves that a smaller step window did not cause significant changes in the overall morphology of signal monitoring. Therefore, it is only necessary to ensure that the frequency of the step is less than the time required for the fast Fourier transform of the window data, and once again, the smaller the frequency of the step, the better. However, reducing the step size is constrained by the calculation time required for the fast Fourier transform on the sampling window.

After extensive analysis, a window size of 1 million data points and a step size of 100 k data points were found to yield better results for this paper with a sampling rate of 200 kHz, as shown in Figure 5. The paper reports the strength of the characteristic signal of the 0–5 s data segment at the 5th second, and the strength of the characteristic frequency spectrum signal of the 0.5–5.5 s data segment at the 5.5th second, and so on, until the end of the welding experiment. To avoid the data vacuum period before the first 5 s, the paper starts data acquisition a few seconds before the arc ignition.

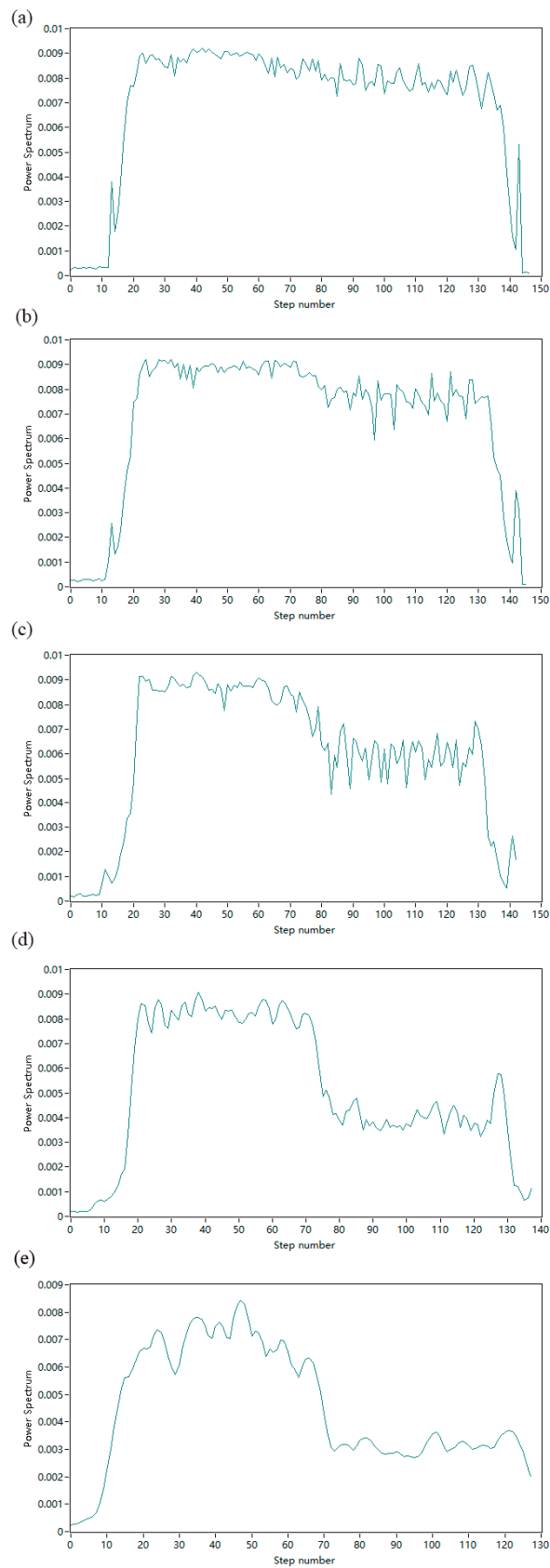


Figure 3. Feature spectrum monitoring images under different data window size: (a) 100 k, (b) 200 k, (c) 500 k, (d) 1 million, (e) 2 million.

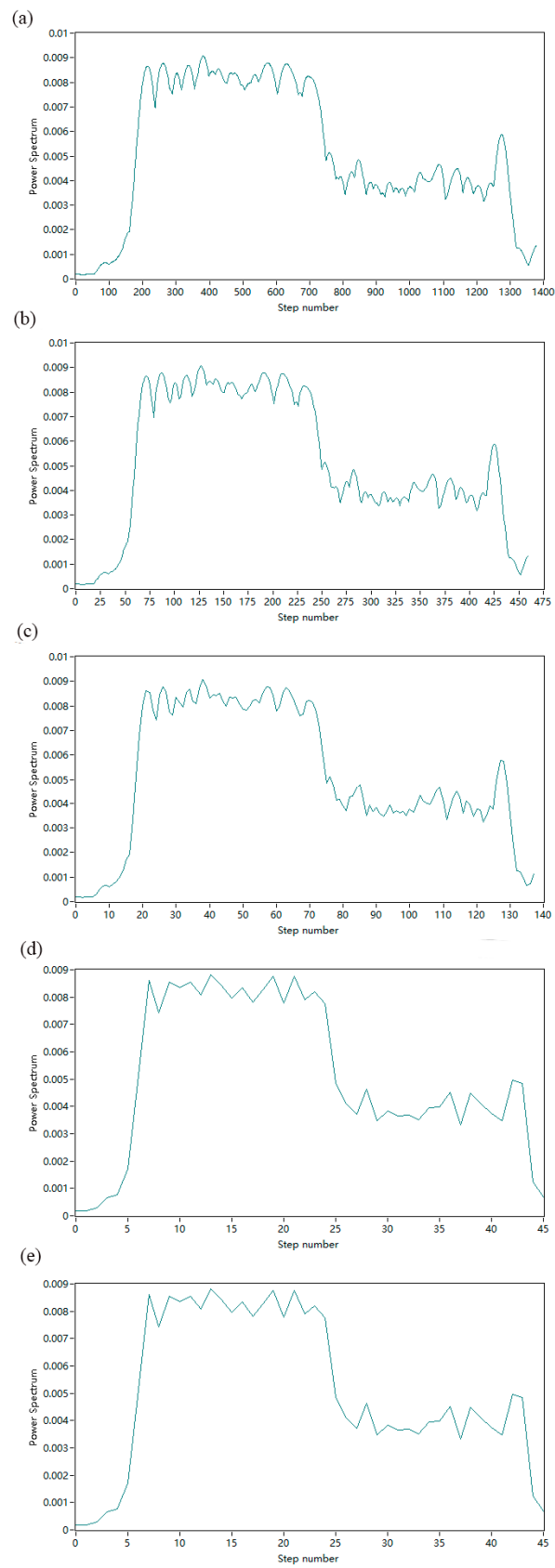


Figure 4. Feature spectrum monitoring images under different data step size: (a) 10 k, (b) 30 k, (c) 100 k, (d) 300 k, (e) 1 million.

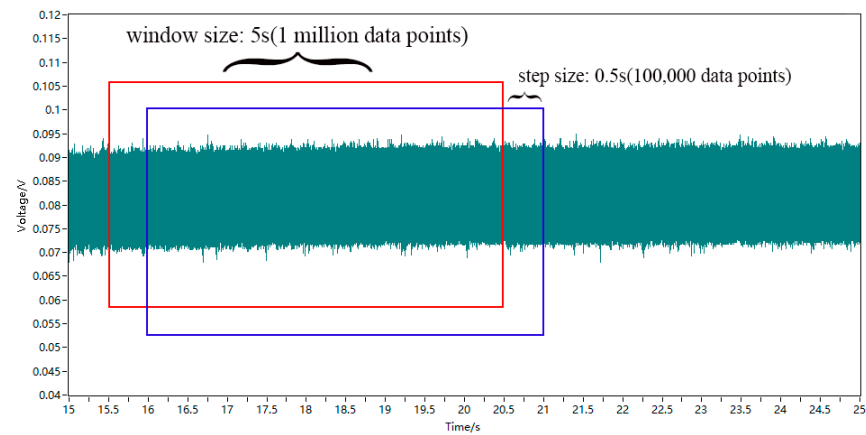


Figure 5. Selection of FFT calculation window and step size.

3.2. Complete and Incomplete Joint Penetration under Steady State

In this paper, we obtained complete joint penetration and incomplete joint penetration welding seams and tracked the characteristic signal strength in the frequency range of 36–37 kHz by adjusting the welding parameters. To this end, welding experiments are conducted and the morphology of the front and back sides of the welding seams is examined and presented in Figure 6a. The welding parameters are adjusted to achieve complete joint penetration at a guaranteed welding speed of 240 mm/min using a welding current of 550 A, followed by incomplete joint penetration using a welding current of 480 A. The voltage time-domain signals collected under two different penetration conditions remain stable, with no visible changes in both. The power spectral tracking graphs of the calculated characteristic signals are plotted and shown in Figure 6b.

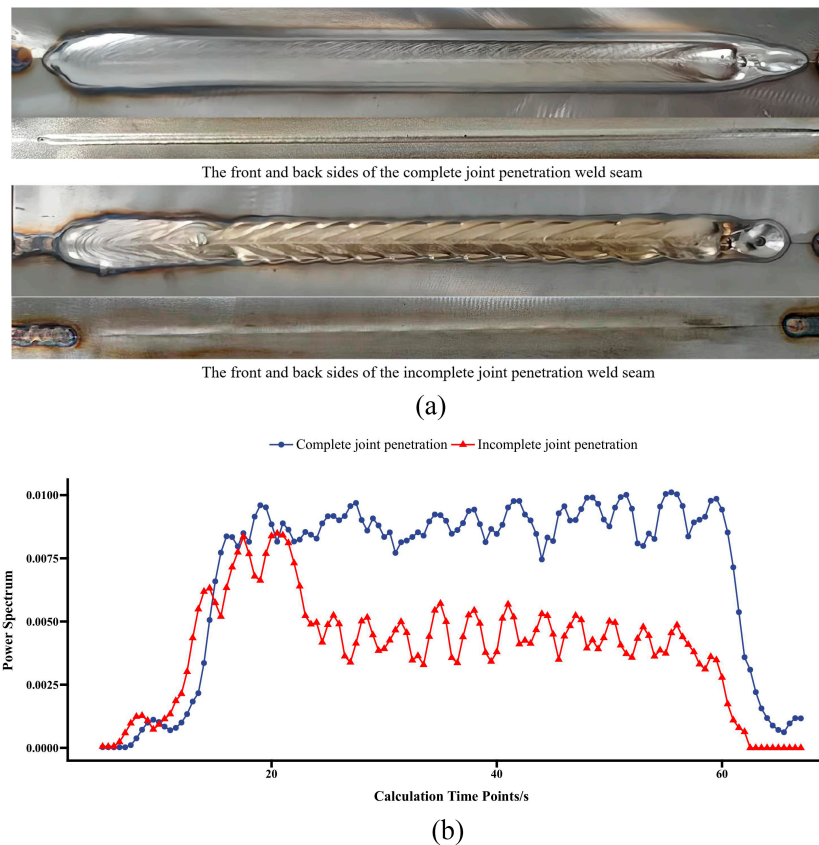


Figure 6. Complete and incomplete joint penetration under steady state. (a) Welding test plate front and back weld beads; (b) monitoring of characteristic signal strength during the welding process.

From Figure 6, it can be observed that the characteristic signal strength in the frequency range of 36–37 kHz in the welding voltage frequency domain signal collected under the two experimental conditions rapidly increased from the arc starting period and then remained relatively stable until it decreased to 0 at the arc ending moment. When the welding melt state did not change during the experiment, the characteristic signal strength remained relatively stable, whether it was in complete joint penetration or incomplete joint penetration. A significantly lower overall strength of the characteristic signal was observed under the incomplete joint penetration state when compared to the characteristic signal strength interval collected under the complete joint penetration state. In-depth research on this characteristic will be conducted in this paper.

3.3. Complete and Incomplete Joint Penetration under Non-Steady State

Notwithstanding the successful acquisition of complete joint penetration and incomplete joint penetration welding seams in Section 3.2, the welding parameters employed are not the same, making it challenging to determine whether the characteristic signal strength is correlated to the welding melt state or independent of the welding parameters. Consequently, this section ensures that the welding parameters remain unaltered while the welding material undergoes a sudden shift in the welding melt state owing to thermal deformation and other factors by selecting the welding parameters at the edge of the welding window: a welding current of 500 A and a welding speed of 240 mm/min. Figure 7 presents the experimental parameters and the morphology of the front and back sides of the welding seams after the experiment, respectively, and depicts the power spectral tracking graph of the calculated characteristic signal. Evidently, as the welding reaches the middle section of the welding seam and the welding melt state changes from complete joint penetration to incomplete joint penetration, the collected characteristic signal strength drops steeply and then stabilizes within a low-intensity interval. This observation confirms that the strength of the characteristic signal is indeed related to the welding melt state and is not unaffected by the unchanged welding parameters.

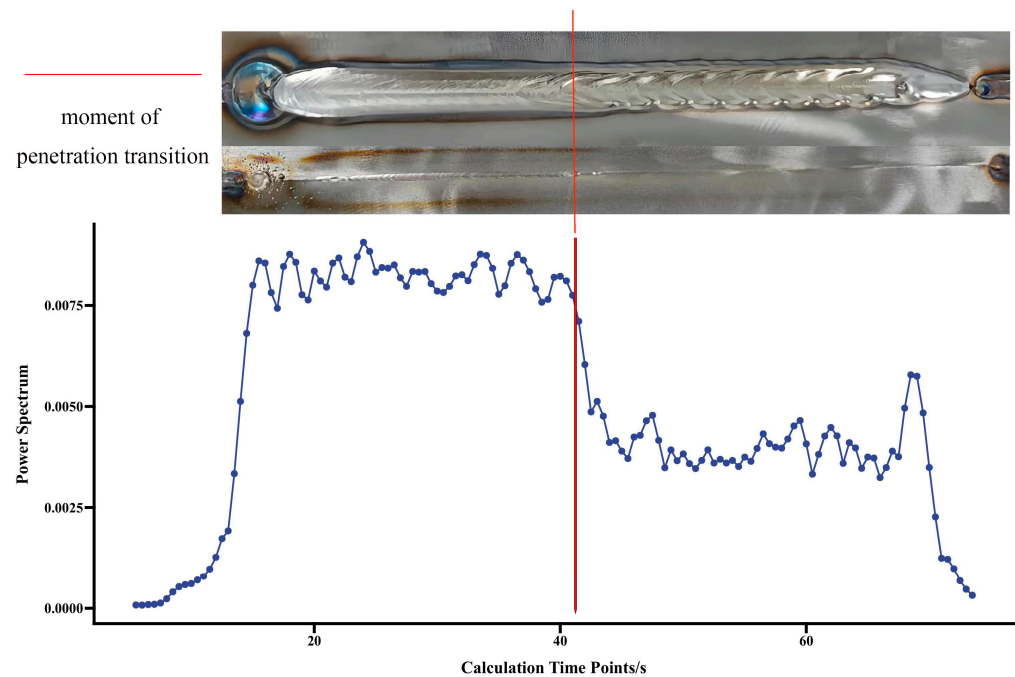


Figure 7. Complete and incomplete joint penetration under the same welding condition.

By monitoring the strength of the characteristic signal, it is possible to judge the welding melt state due to the unique characteristics of the signal. This paper proposes the possibility of achieving closed-loop control and ensuring welding quality stability by

continuously adjusting the welding parameters to maintain the strength of the characteristic signal in the complete joint penetration interval or returning to the complete joint penetration state when incomplete joint penetration occurs. However, this assumption is based on two prerequisites. Firstly, when the welding melt state changes from complete joint penetration to incomplete joint penetration and the strength of the characteristic signal drops, adjusting the welding parameters to return to the complete joint penetration state will lead to a rise in the strength of the characteristic signal. Secondly, adjusting the welding parameters will not significantly impact the strength of the characteristic signal.

3.4. Analysis

The welding power source employed in this study is an inverter arc welding power source that utilizes high-frequency inverter technology to convert a direct current source into a high-frequency alternating current source. The resulting alternating current is then stepped down through a transformer and rectified to obtain the desired direct current source. During this process, a certain amount of intermediate frequency alternating current component is generated, which coincides with the intermediate frequency alternating current signal collected at 36–37 kHz, owing to the switching frequency of the inverter being typically between 10 kHz and 100 kHz.

In the event of a transition from complete joint penetration to incomplete joint penetration during welding, the unstable state of the weld pool is attributed to the inability to form a stable keyhole, leading to instability in the weld pool, such as the occurrence of weld pool rolling, which, in turn, causes instability in the arc state. In the inverter arc welding circuit, an electronic switch is utilized as a method of controlling the arc current, which can adjust the duty cycle and frequency of the arc current. When the arc is unstable, the electronic switch needs to adjust the arc current to maintain stability, causing changes in the intensity of the intermediate frequency component in the arc current.

Existing theories have shown that changes in arc length lead to changes in arc resistance and conductivity, thereby affecting the waveform and spectrum of the arc current and voltage. Consequently, changes in the welding molten state result in changes in the power spectrum intensity of the intermediate frequency alternating current signal at 36–37 kHz.

4. Verification

To further verify the potential influence and monitoring capability of the characteristic frequency and strength of arc voltage on the welding melt state, the present study manipulates the welding speed during the welding process to modulate the heat input and obtain diverse melting states. To ensure welding-current consistency, it is imperative to have a constant rate of 525 A. In the first experiment, incomplete joint penetration occurred during welding due to current increments in the step state. The penetration state was eventually restored as the welding speed decreased after a certain period of time. In the second experiment, welding current was increased periodically, resulting in both a dynamic welding condition that maintained the penetration state and a dynamic welding condition that altered the penetration state. Both conditions were subjected to data collection and subsequent analysis. Figures 8 and 9 depict the front and back sides of the welding seam and the power spectrum intensity tracking of characteristic signals.

This study demonstrates the possibility of transforming the incomplete joint penetration state, which occurs during the welding process, into a normal melt state by adjusting the welding speed. Moreover, the transformation process can be characterized and evaluated by monitoring the strength change of the characteristic frequency spectrum signal. The experiment confirms the feasibility of closed-loop control of welding quality by monitoring the strength of the characteristic frequency spectrum signal of the welding electrical signal. Specifically, when the welding parameters are adjusted without changing the melt state, the monitored characteristic frequency spectrum signal remains unchanged. However, when the welding parameters are adjusted to alter the welding melt state, a transformation of the characteristic frequency spectrum signal can be observed. Therefore, by monitoring

the characteristic frequency spectrum signal and adjusting the welding parameters, it is possible to maintain the welding process in a complete joint penetration state and achieve closed-loop control of welding melt quality. This approach provides a reliable method for enhancing the consistency and stability of welding melt quality and improving the efficiency of welding production.

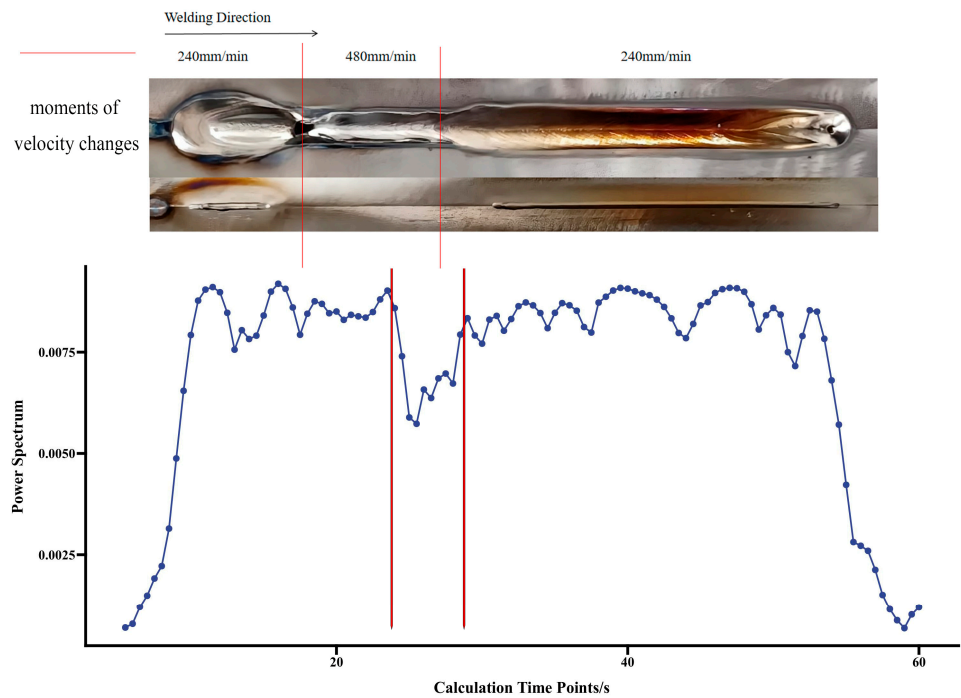


Figure 8. Power spectrum intensity tracking of characteristic signals under step change of the welding speed.

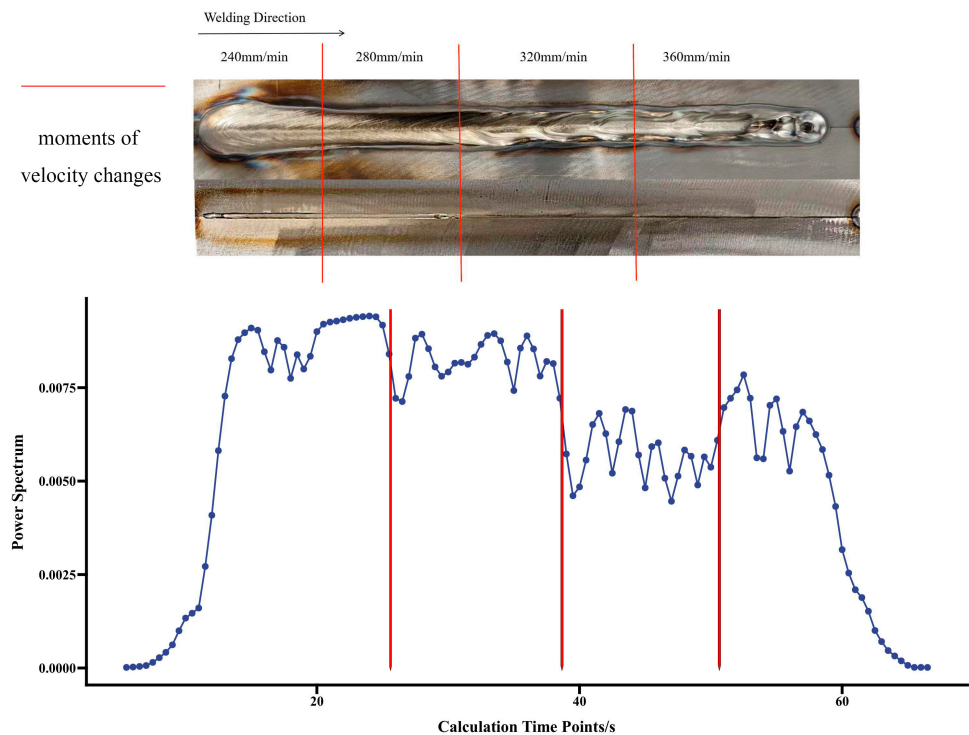


Figure 9. Power spectrum intensity tracking of characteristic signals under step increase of the welding speed.

5. Conclusions

Through an experimental investigation of austenitic 304 stainless steel, this study draws several conclusions based on the analysis of experimental results and verification outcomes.

Firstly, an acquisition system is established to collect voltage and current signals during the welding process, and the welding signals are obtained through the docking welding experiments. A significant frequency spectrum segment is discovered at 36–37 kHz, which represents different welding melt states, including complete joint penetration and incomplete joint penetration states.

Secondly, the characteristic signal strength of the 36–37 kHz frequency spectrum segment is significantly higher in the complete joint penetration state than in the incomplete joint penetration state. Furthermore, when the melt state has no observable changes, the characteristic signal strength remains relatively stable and does not change a lot due to changes in welding parameters. However, when the melt state changes in a visible manner from complete joint penetration to incomplete joint penetration, the characteristic signal strength will decrease observably.

Thirdly, the characteristic signal strength will increase again to the initial complete joint penetration state's characteristic signal strength range by adjusting the compensation parameters to re-transform it into a complete joint penetration state when the welding changes from complete joint penetration to incomplete joint penetration.

Based on these findings, this study proposes that the characteristic signal strength is only related to the melt state and does not change with changes in welding parameters. By monitoring the characteristic frequency spectrum signal and adjusting the welding parameters, the welding process can be maintained in a complete joint penetration state, thus achieving closed-loop control of welding melt quality. This approach may be beneficial in improving the consistency and stability of welding melt quality and enhancing the efficiency of welding production.

Author Contributions: Conceptualization, R.Y.; methodology, G.X.; software, H.B. and N.N.; validation, G.X. and H.B.; data curation, H.B.; writing—original draft preparation, H.B. writing—review and editing, N.N.; supervision, Y.W.; project administration, R.Y. and Y.W. All authors have read and agreed to the published version of the manuscript.

Funding: This research received no external funding.

Data Availability Statement: Data sharing not applicable.

Conflicts of Interest: The authors declare that they have no known competing financial interests or personal relationships that could have appeared to influence the work reported in this paper.

References

1. Lathabai, S.; Jarvis, B.L.; Barton, K.J. Comparison of keyhole and conventional gas tungsten arc welds in commercially pure titanium. *Mater. Sci. Eng. A* **2001**, *299*, 81–93. [[CrossRef](#)]
2. Jarvis, B.L. Keyhole Gas Tungsten Arc Welding: A New Process Variant. Ph.D. Thesis, University of Wollongong, Wollongong, Australia, 2001.
3. Liu, Z.; Fang, Y.; Cui, S.; Yi, S.; Qiu, J.; Jiang, Q.; Liu, W.; Luo, Z. Sustaining the open keyhole in slow-falling current edge during K-TIG process: Principle and parameters. *Int. J. Heat Mass Transf.* **2017**, *112*, 255–266. [[CrossRef](#)]
4. Liu, Z.; Chen, S.; Yuan, X.; Zuo, A.; Zhang, T.; Luo, Z. Magnetic-enhanced keyhole TIG welding process. *Int. J. Adv. Manuf. Technol.* **2018**, *99*, 275–285. [[CrossRef](#)]
5. Cui, S.L.; Liu, Z.M.; Fang, Y.X.; Luo, Z.; Manladan, S.M.; Yi, S. Keyhole process in K-TIG welding on 4 mm thick 304 stainless steel. *J. Mater. Process. Technol.* **2017**, *243*, 217–228. [[CrossRef](#)]
6. Cui, S.W.; Shi, Y.H.; Sun, K.; Gu, S. Microstructure evolution and mechanical properties of keyhole deep penetration TIG welds of S32101 duplex stainless steel. *Mater. Sci. Eng. A* **2018**, *709*, 214–222. [[CrossRef](#)]
7. Shi, Y.H.; Cui, S.W.; Zhu, T.; Gu, S.; Shen, X. Microstructure and intergranular corrosion behavior of HAZ in DP-TIG welded DSS joints. *J. Mater. Process. Technol.* **2018**, *256*, 254–261. [[CrossRef](#)]
8. Cui, S.W.; Shi, Y.H.; Cui, Y.X.; Zhu, T. The impact toughness of novel keyhole TIG welded duplex stainless steel joints. *Eng. Fail. Anal.* **2018**, *94*, 226–231. [[CrossRef](#)]
9. Saad, E.; Wang, H.; Kovacevic, R. Classification of molten pool modes in variable polarity plasma arc welding based on acoustic signature. *J. Mater. Process. Technol.* **2006**, *174*, 127–136. [[CrossRef](#)]

10. Wang, H.; Kovacevic, R. Feasibility study of acoustic sensing for the welding pool mode in variable-polarity plasma arc welding. *Proc. Inst. Mech. Eng. Part B J. Eng. Manuf.* **2002**, *216*, 1355–1366. [[CrossRef](#)]
11. Cayo, E.H.; Alfaro, S. A Non-Intrusive GMA Welding Process Quality Monitoring System Using Acoustic Sensing. *Sensors* **2009**, *9*, 7150–7166. [[CrossRef](#)]
12. Ferrara, M.; Ancona, A.; Lugara, P.M.; Sibilano, M. Online quality monitoring of welding processes by means of plasma optical spectroscopy. *Proc. SPIE* **2000**, *3888*, 750–758.
13. Garcia-Allende, P.B.; Mirapeix, J.; Conde, O.M.; Cobo, A.; Higuera, J.M.L. Spectral processing technique based on feature selection and artificial neural networks for arc-welding quality monitoring. *NDT E Int.* **2009**, *42*, 56–63. [[CrossRef](#)]
14. Zhang, Z.-F.; Zhong, J.-Y.; Chen, Y.-X.; Chen, S.-B. Online welding quality monitoring based on feature extraction of arc voltage signal. *Int. J. Adv. Manuf. Technol.* **2014**, *70*, 1661–1671. [[CrossRef](#)]
15. Jager, M.; Hamprecht, F.A. Principal Component Imagery for the Quality Monitoring of Dynamic Laser Welding Processes. *IEEE Trans. Ind. Electron.* **2009**, *56*, 1307–1313. [[CrossRef](#)]
16. Wang, X.J.; Zhou, J.H.; Yan, H.C.; Pang, C.K. Quality monitoring of spot welding with advanced signal processing and data-driven techniques. *Trans. Inst. Meas. Control.* **2018**, *40*, 2291–2302. [[CrossRef](#)]
17. Huang, J.; Shi, Y.; Lu, L.; Ding, F. Modeling, Simulation Analysis and Arc Length Control of Pulsed MIG Welding. *J. Mech. Eng.* **2011**, *47*, 37–41. [[CrossRef](#)]
18. Zhang, Z.; Chen, H.; Xu, Y.; Zhong, J.; Lv, N.; Chen, S. Multisensor-based real-time quality monitoring by means of feature extraction, selection and modeling for Al alloy in arc welding. *Mech. Syst. Signal Process.* **2015**, *60–61*, 151–165. [[CrossRef](#)]
19. Simmen, K.; Buch, B.; Breitbarth, A.; Notni, G. Multimodal Image Acquisition and Processing System for In-line Quality Monitoring of Welding Processes. In Proceedings of the Young Welding Professionals International Conference, Halle, Germany, 16–18 August 2017.
20. Cai, W.; Wang, J.; Jiang, P.; Cao, L.; Mi, G.; Zhou, Q. Application of sensing techniques and artificial intelligence-based methods to laser welding real-time monitoring: A critical review of recent literature. *J. Manuf. Syst.* **2020**, *57*, 1–18. [[CrossRef](#)]
21. Trushnikov, D.; Krotova, E.; Koleva, E. Use of a secondary current sensor in plasma during electron-beam welding with focus scanning for process control. *J. Sens.* **2016**, *2016*, 1–13. [[CrossRef](#)]
22. Cui, Y.; Shi, Y.; Zhu, T.; Cui, S. Welding penetration recognition based on arc sound and electrical signals in K-TIG welding. *Measurement* **2020**, *163*, 107966. [[CrossRef](#)]
23. Chen, Q.; Sun, Z.; Sun, J.; Wang, Y. Closed-loop control of weld penetration in keyhole plasma arc welding. *Trans. Nonferrous Met. Soc. China* **2004**, *14*, 116–120. [[CrossRef](#)]
24. Huang, J.; Yang, M.; Chen, J.; Yang, F.; Zhang, Y.; Fan, D. The oscillation of stationary weld pool surface in the GTA welding. *J. Mater. Process Technol.* **2018**, *256*, 57–68. [[CrossRef](#)]
25. Cui, Y.; Shi, Y.; Hong, X. Analysis of the frequency features of arc voltage and its application to the recognition of welding penetration in K-TIG welding. *J. Manuf. Process.* **2019**, *46*, 225–233. [[CrossRef](#)]

Disclaimer/Publisher’s Note: The statements, opinions and data contained in all publications are solely those of the individual author(s) and contributor(s) and not of MDPI and/or the editor(s). MDPI and/or the editor(s) disclaim responsibility for any injury to people or property resulting from any ideas, methods, instructions or products referred to in the content.